

## Dopant Effect and Characterization of Poly (O-Toluidine)/Vanadium Pentoxide Composites Prepared by in Situ Polymerization Process

Shama Islam<sup>1</sup>, Mohsin Ganaie<sup>1</sup>, Shabir Ahmad<sup>1</sup>, Azher M. Siddiqui<sup>1</sup> and M. Zulfequar<sup>2</sup>

### Abstract

---

Conducting polymer composites of poly o-toluidine/vanadium pentoxide (POT/V<sub>2</sub>O<sub>5</sub>) were synthesized by polymerization of o-toluidine with V<sub>2</sub>O<sub>5</sub> using (NH<sub>4</sub>)<sub>2</sub> S<sub>2</sub>O<sub>8</sub>) as an oxidant. The V<sub>2</sub>O<sub>5</sub> is varied in five different weight percentages of POT in POT/V<sub>2</sub>O<sub>5</sub> composites. The synthesized polymer composites are characterized by dc conductivity; UV-Visible absorption spectroscopy, FTIR, Photoluminescence and XRD techniques. Electrical conductivity of the compressed pellets depends on the concentration of V<sub>2</sub>O<sub>5</sub> in POT. The optical band gap of composites decreases with increase in the weight percent of V<sub>2</sub>O<sub>5</sub>. X-ray diffraction pattern shows increases in the crystallinity which is due to interaction of POT with V<sub>2</sub>O<sub>5</sub>. The PL emission intensity of all the polymer/V<sub>2</sub>O<sub>5</sub> composites makes them suitable for various optoelectronic devices.

---

**Keywords:** Optical properties/techniques, Chemical properties, Defects, Electrical properties, Powder processing

### 1. Introduction

Conducting polymers have emerged as a very important class of materials because of their unique electrical, optical and chemical properties leading to the wide range of technological applications.

This class of materials provides tremendous scope for tuning of their electrical conductivity from semiconducting to metallic regime by way of doping [1, 2].

---

<sup>1</sup> Department of Physics, Jamia Millia Islamia, New Delhi-110025, India.

<sup>2</sup> Prof. and Head, Department of Physics, Faculty of Natural Science, Jamia Millia Islamia, New Delhi -110025, India. E-mail: mzulfe@rediffmail.com, Phone: - 91-11-26989965

The unique properties of conducting polymers have led to the development of new models to explain their observed properties, particularly various mechanisms of charge transport [3, 4]. Among all conducting polymers, polyaniline is one of the most promising conducting polymers; but this is inherently brittle and has poor processibility, due to the insolubility in common organic solvents [5-7]. This problem has been overcome to some extent by using substituted derivatives of anilines such as o-toluidines, anisidines, N-methyl or N-ethyl anilines etc. [8-10]. In order to obtain additional insight into polyaniline, a methyl substituent has been used to block the *ortho* position of aromatic ring of aniline. It may be remarked that methyl-substituted aniline called o-toluidines has been found to have additional advantage over polyaniline due to its fast switching time between the oxidized and reduced states. POT was chosen as the conducting polymer owing to its higher processibility as well as solubility as compared with PANI [11].

The composite materials based on electrically conductive polymers have attracted the attention of investigators for the development of new functional materials [12-15]. The reason for such interest is that materials of this type frequently manifest properties that cannot be achieved by the individual components. These compounds have great potential for their use in chemical current sources, photocatalytic and electro-catalytic systems and as dopant additions for enhancement of quantum yield in these devices.

However, when they are taken in the composite form their electrical as well as dielectric properties are altered from those of basic materials. A number of groups have reported studies on the electrical conductivity and dielectric properties of composites of a variety of conducting polymers [16, 17]. It has been shown that the conductivity of these heterogeneous systems depends on many factors such as the concentration of conducting fillers, their shape, size, orientation and interfacial interaction between filler molecules and host matrix. In case of conducting polymers as fillers, the degree of cross-linking between the polymeric chains also affects the electrical properties in these composites [18-19].

The aim of our work is to enhance the properties of POT by using a dopant. Among inorganic compounds as dopant  $V_2O_5$  is of prime importance because of its proven use in electronics [19, 20].

$V_2O_5$  exhibits photovoltaic action, where light is converted directly into electricity and photoconductive action where electrical resistance decreases with increased illumination. It is a Lewis acid, which makes it a suitable candidate for the doping of conducting polymers. Moreover,  $V_2O_5$  is stable and has no hazardous effects and is easy to manipulate. It has been reported that  $V_2O_5$  can remarkably improve the current efficiency of Organic field-effect transistors and OLEDs [21–23].  $V_2O_5$  has found various applications in sensor and electrochromic devices, lithium batteries, catalysts, etc.

In the present paper, we report the synthesis of POT by chemical oxidation polymerization in aqueous medium and POT/ $V_2O_5$  composites with five different weight percentage of  $V_2O_5$ . DC conductivity measurements have been done for undoped POT and POT/ $V_2O_5$  composites separately. The composites are characterized by UV-Visible studies and XRD. FTIR studies have also been performed to study the structural changes due to the incorporation of dopant into polymeric chain. Photoluminescence (PL) studies of the materials were also observed.

## 2. Experimental

All chemicals used were of analytical reagent (AR) grade. The monomer o-toluidine was distilled prior to use. Ammonium persulphate ( $(NH_4)_2 S_2O_8$ ), hydrochloric acid (HCl) and Vanadium pentoxide  $V_2O_5$  were used as received in the present study.

Chemically polymerized POT and its Vanadium pentoxide composites were obtained by oxidative polymerization by using  $(NH_4)_2 S_2O_8$  as oxidant in aqueous medium. 0.1 mol of o-toluidine was dissolved in 1 M HCl. To this reaction mixture, 0.1 M solution of ammonium persulphate was added slowly with continuous stirring for 4–6 h at 0–5°C. As soon as the o-toluidine mixed with the  $(NH_4)_2 S_2O_8$  solution, it turned to characteristic dark green colour, indicating that the organic polymerization reaction began immediately. The hybrid of solid oxide and POT was filtered and washed thoroughly with water. Finally, the resultant precipitate was dried in an oven for 24 h to achieve a constant weight. To remove last traces of unreacted POT, it was then washed with tetrahydrofuran. The oxide was varied in weight percentages (10, 20, 30, 40 and 50%) dissolved in water and added to the POT solution with vigorous stirring in order to keep the vanadium pentoxide suspended in the solution.

This approach promotes molecular level mixing of precursor and the polymerization of initiators of both networks. All the composites were filtered and dried in an oven for 24 h and vacuum dried at 60–70° C for 1 h. These composites were then characterized by different techniques.

DC conductivity of all the polymer composites was measured by using two-probe technique in the temperature range 305 - 470K. For measuring DC conductivity, bulk samples in the form of pellets were obtained by finely grinding the polymer powder and then compressing it under a pressure of 6.2 ton. A voltage of 1.5 V (DC) was applied across the pellet and resulting current was measured with a Keithley electrometer Model 6157A. The pellets were mounted between the two steel electrodes inside a metallic sample holder. The temperature was measured with a calibrated copper–constantan thermo couple mounted near the electrodes [24-26].

For information about the crystallinity, X-ray diffraction (XRD) studies have been carried out by using a panalytical (PW 3710) X-ray powder diffractometer with Cu K $\alpha$  radiation. The sample is scanned in angular range of 0–700 with scan speed of 0.010/s under similar conditions. UV–Visible Spectroscopy of the samples has been carried out using Camspec M550 double beam UV–Visible Spectrophotometer. FTIR spectra of undoped and doped pellets were obtained by using Perkin Elmer FTIR spectrometer in the range from 400 cm<sup>-1</sup> to 4000 cm<sup>-1</sup>.

### 3. Results and Discussion

#### 3.1. Dc Conductivity Studies

The electrical conductivity of conducting polymers results from mobile charge carriers introduced into the  $\pi$ -electronic system through doping [27]. The DC conductivity ( $\sigma_{dc}$ ) of all the polymer composites in a temperature range of 305 - 470K is studied at a constant voltage of 1.5V. The conductivity as a function of temperature can be represented by the relation [25, 26]

$$\sigma_{dc} = \sigma_0 \exp\left(\frac{\Delta E_a}{kT}\right) \quad (1)$$

Here  $\Delta E_a$  is the activation energy,  $\sigma_0$  is the pre exponential factor related to the material,  $k$  is Boltzmann constant and  $T$  is the temperature.

Arrhenius plots of conductivity of undoped and doped POT with different weight percentage of  $V_2O_5$  are shown in Figure 1. The value of the activation energy ( $\Delta Ea$ ) is estimated with the help of the slope of  $\ln\sigma_{dc}$  versus  $1000/T$  plot and using a linear fit. The plots are straight lines, which indicate that conduction in these samples is through an activated process; the change in slope is responsible for the change in activation energy. As the slope of the graph increases with the dopant concentration, DC conductivity and the activation energy increases. Further, the slope of the graph explains the conductivity mechanism taking place in the doped POT samples.

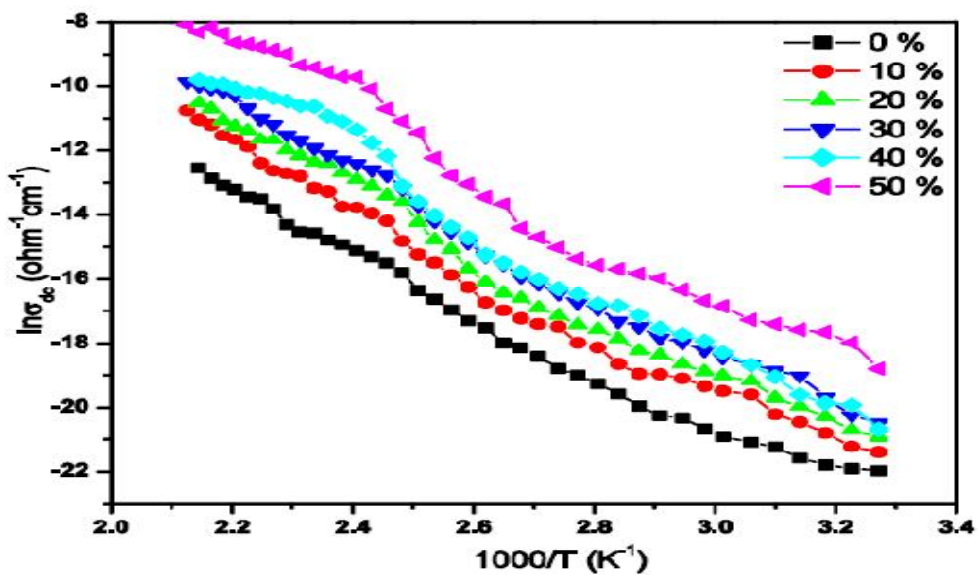


**Figure 1: Temperature Dependent DC Conductivity in the Temperature Range (305 K–470 K) of POT/  $V_2O_5$  Composites with different Weight Percentage of  $V_2O_5$**

Doping introduces charge carriers into the electronic structure. The attraction of an electron in one repeated unit to the nuclei of the neighboring unit leads to carrier delocalization along the polymer chain. Thus, doping of  $V_2O_5$  implies charge transfer, the associated insertion of a counter ion and the simultaneous control of Fermi level or chemical potential. As a result, the conductivity increases because of an increase in carrier concentration with doping, which ultimately enhances the mobility of charge carrier. When  $V_2O_5$  is doped with 40 and 50 wt %, sudden increase in conductivity and broadening of PL spectrum peak are observed.

Thus,  $V_2O_5$  doped POT at these particular doping percentages, can be used for sensor purposes. The variation of  $\sigma_{dc}$  and  $\Delta E_a$  with concentration of dopant are shown in Figures 2.

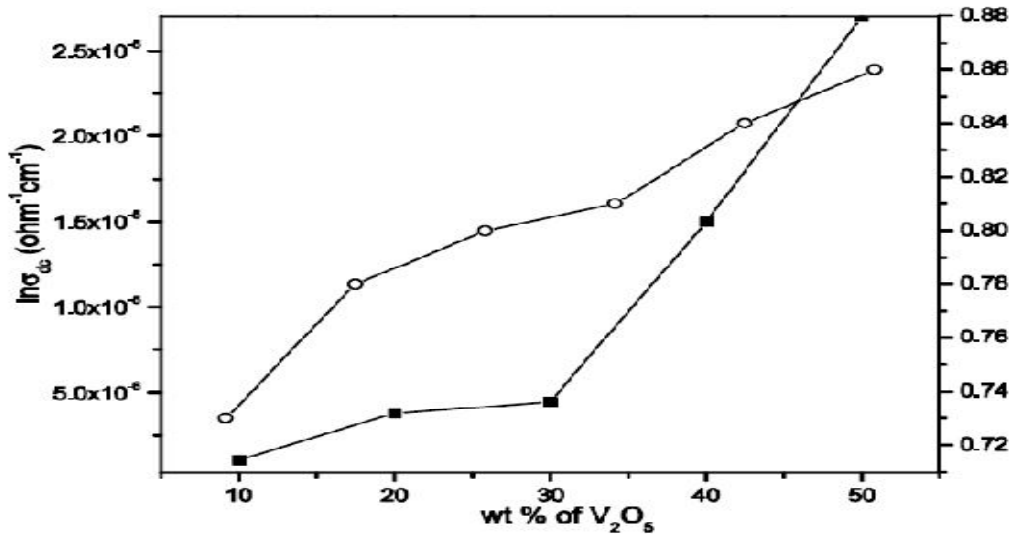


**Figure 2: The Plot of DC Conductivity and Activation Energy vs. Weight Percentage of V2O5**

This figure shows that, the initial increase in activation energy with the increase of dopant concentration might be due to the increase of charge carrier concentration and the Fermi level may change. The activation energy alone does not indicate that the mechanism of conductivity is taking place in extended states above the mobility edge or by the hopping in localized states. For obtaining a distinction between these mechanisms, Davis and Mott suggested that the pre exponential factor for conduction in extended states should be two or three orders greater than the conduction in localized states [28]. The magnitude of pre exponential factor lies in the range of  $10^3$ - $10^4$   $ohm^{-1}cm^{-1}$  which shows that the conduction is due to the excitation of charge carriers into the extended states. Also, the conduction is taking place by hopping process because of the wide range of localized states present near the Fermi level. Thus conduction through extended states is completely ruled out. The value of activation energy, DC conductivity ( $\sigma_{dc}$ ) and pre exponential factor ( $\sigma_0$ ) are given in table 1.

Sample	$E_g$ (eV)	$\alpha(\text{cm}^{-1})$	$\epsilon'$	$\epsilon''$	n	$\Delta E_a$ (eV)	$\sigma_{dc} (\Omega^{-1}\text{cm}^{-1})$	$\sigma_o (\Omega^{-1}\text{cm}^{-1})$
POT/V2O5 0%	1.77	2.20939	$2.28 \times 10^4$	7.57	8.34	0.73	$3.30 \times 10^{-7}$	$.197 \times 10^3$
POT/V2O5 10%	1.58	1.42505	$1.35 \times 10^5$	55.23	13.09	0.78	$1.08 \times 10^{-6}$	$5.54 \times 10^3$
POT/V2O5 20%	1.52	2.68651	$1.40 \times 10^5$	56.45	54.78	0.80	$3.80 \times 10^{-6}$	$27.93 \times 10^3$
POT/V2O5 30%	1.47	1.75203	$1.40 \times 10^5$	56.54	30.99	0.81	$4.50 \times 10^{-6}$	$54.30 \times 10^3$
POT/V2O5 40%	1.42	2.69324	$1.39 \times 10^5$	56.34	32.39	0.84	$1.52 \times 10^{-5}$	$292.80 \times 0^3$
POT/V2O5 50%	1.25	2.68786	$1.39 \times 10^5$	56.33	128.06	0.86	$2.70 \times 10^{-5}$	$3040 \times 10^3$

**Table 1:** Variation of activation energy ( $\Delta E_a$ ), DC conductivity ( $\sigma_{dc}$ ), pre-exponential factor ( $\sigma_o$ ) and Indirect band gap ( $E_g$ ), absorption coefficient ( $\alpha$ ), real part of dielectric constant ( $\epsilon'$ ), imaginary part of dielectric constant ( $\epsilon''$ ), refractive index (n) with different concentration of V2O5 in POT at 450 K, 620 nm

### 3.2. UV-Visible and Dielectric Studies

UV-Visible absorption spectra of the undoped and doped POT are shown in Figure 3, which clearly indicates that the absorption intensity increases after doping. The peak at 487 nm which corresponds to  $\pi$ - $\pi^*$  transition of fully oxidized phase indicates the occurrence of emeraldine salt form of POT. This peak shifts towards the higher wavelength corresponding to red shift in doped samples. This fact is also confirmed by the increase in conductivity up to 50% doped sample [30].

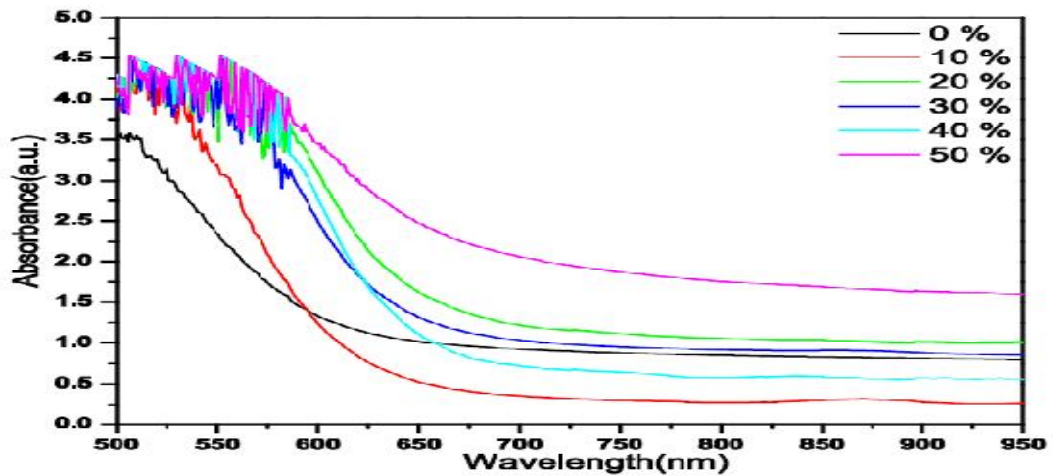


**Figure 3: UV-Visible Absorption Spectra of POT/ V<sub>2</sub>O<sub>5</sub> Composites with different Weight Percentage of V<sub>2</sub>O<sub>5</sub>**

From UV-Visible absorption spectrum the optical band gap has been measured using Tauc's relation [23, 24],

$$(\alpha h\nu) \propto (h\nu - E_g)^n \text{ where } n=1,2,3,\dots \quad (2)$$

The index  $n$  has discrete values like  $1/2$ ,  $3/2$ ,  $2$  or more depending on whether the transition is direct or indirect and allowed or forbidden, respectively. In the direct and allowed cases, the index  $n$  is  $1/2$  whereas for the direct but forbidden cases it is  $3/2$ . But for the indirect and allowed cases  $n=2$  and for the forbidden cases it will be  $3$  or more. The present system obeys the rule of indirect transition with  $n=2$ .  $\square$  is given by,

$$\alpha = O_d/t,$$

where  $O_d$  is the optical density measured at a given film thickness ( $t$ ), and the extinction coefficient ( $k$ ) is given by

$$k = \alpha\lambda / 4\pi,$$

where  $\lambda$  is wavelength of incident photon. The optical band gap of doped and undoped samples has been measured by plotting  $(\alpha h\nu)^{1/2}$  versus energy [29]. The optical band gap has been found to decrease with increase weight percentage of V<sub>2</sub>O<sub>5</sub>. The decrease in band gap may occur due to broadening of polaron bands, which is attributed to the increase in carrier concentration in the polymer composites. The increase in conjugation also leads to decrease in the optical band gap. The difference between the optical band gap and electronic band gap (activation energy) is due to the indirect transition in the system during optical analysis. This transition has two step process in which electron absorbs both photon and phonon. Here photon supplies the needed energy and the phonon supplies the momentum. But the activation energy is the energy required to excite the electron from valence band to conduction band. So the optical band gap value is always greater than the electronic band gap [30, 31].

The UV-visible reflection spectrum is given in Figure 4. From reflection and absorption spectra the refractive index, dielectric constant and dielectric loss in the visible region were measured. The refractive index (n) has been determined by using following relation

$$R = \frac{[(n-1)^2 + k^2]}{[(n+1)^2 + k^2]}$$

The values of dielectric constant ( $\epsilon'$ ) and dielectric loss ( $\epsilon''$ ) are estimated by using the following relations [25]

$$\epsilon' = n^2 - k^2$$

$$\text{and } \epsilon'' = 2nk$$

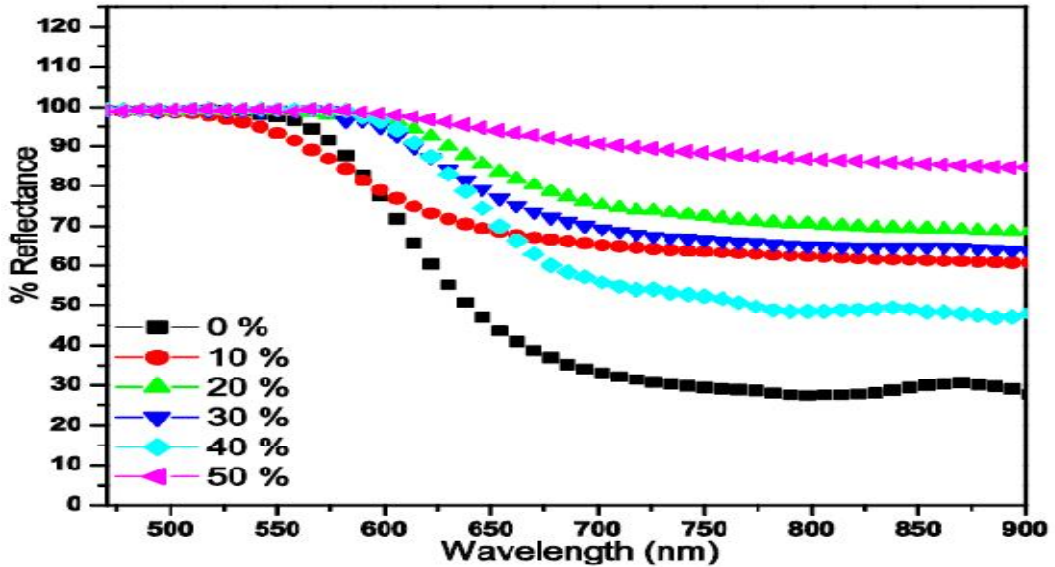


**Figure 4: UV-Visible Reflection Spectra of POT/  $V_2O_5$  Composites at different Weight Percentage of  $V_2O_5$**

The optical parameters have been plotted versus photon energy in figures 5 (a, b). It is clear from these figures that the refractive index and dielectric constant of POT/ $V_2O_5$  composites increase exponentially with photon energy. Higher dielectric constant and dielectric loss for higher content of oxide, which may be due to increase in oxide, increases the crystallinity (as revealed from XRD). As a result orderliness increases the interfacial interactions between the polymer and  $V_2O_5$  leading to maximum space charge polarization. The dielectric constant arises due to static dielectric permittivity, which can be given as

$$\epsilon_s = C_{gb}/C_0$$

The above equation demonstrates that the dielectric constant mainly depends on the grain boundary capacitance( $C_{gb}$ ).

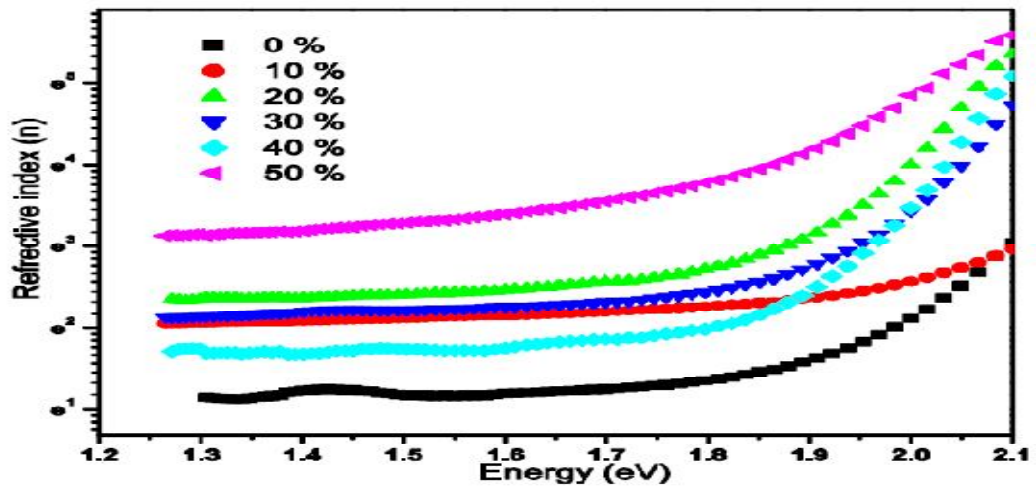


Figure 5(a): The Refractive Index of POT/  $V_2O_5$  Composites at different Weight Percentage of  $V_2O_5$

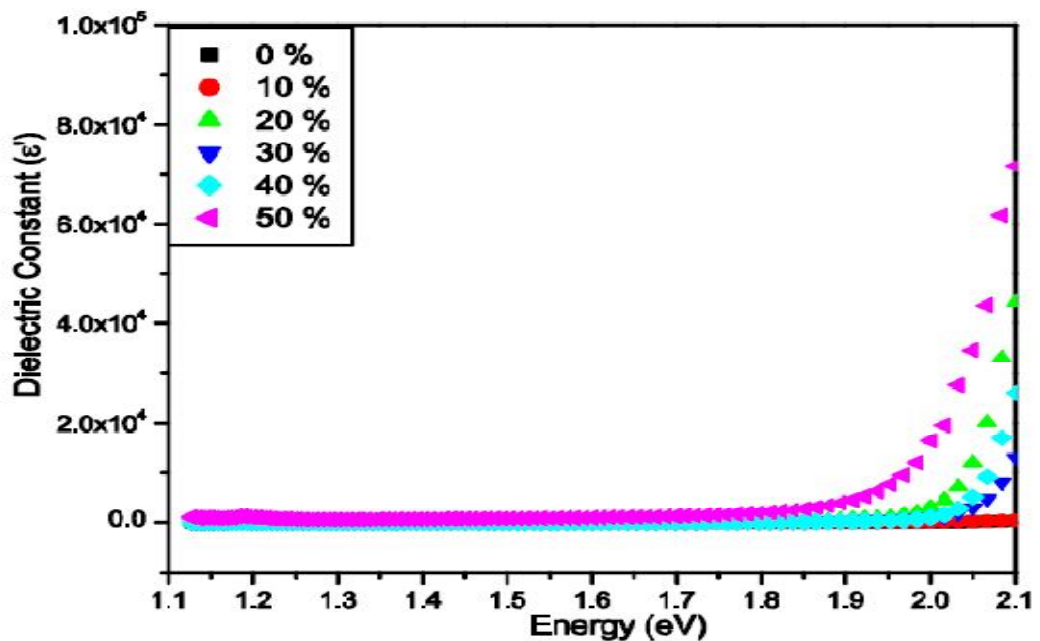


Figure 5(b): The Dielectric Constant of POT/  $V_2O_5$  Composites at different Weight Percentage of  $V_2O_5$

The grain conductivity decreases with increase in V<sub>2</sub>O<sub>5</sub> concentration, the charge carrier concentration decreases resulting in a decrease in grain boundary capacitance. The grain size also decreases with increasing V<sub>2</sub>O<sub>5</sub> content. Hence the reduction of grain boundary capacitance and grain size gives rise to a decrease in dielectric constant. In case of composites, while oxide content is less (i.e. 10%) in the polymer the interface between the polymer and grain is poor leading to decrease in conductivity and dielectric behaviour. There is no change in the dielectric constant in visible region. The change observed only in UV region [31].

### 3.3. FTIR Studies

From FTIR spectra we can observe a change in the functional groups. In these spectra, the region from 0 to 1000 cm<sup>-1</sup> is the finger print region and 1000 cm<sup>-1</sup> to 4500 cm<sup>-1</sup> is the functional group region. Figure 6 shows FTIR spectra of undoped POT and POT doped with V<sub>2</sub>O<sub>5</sub> in different compositions (w/w).

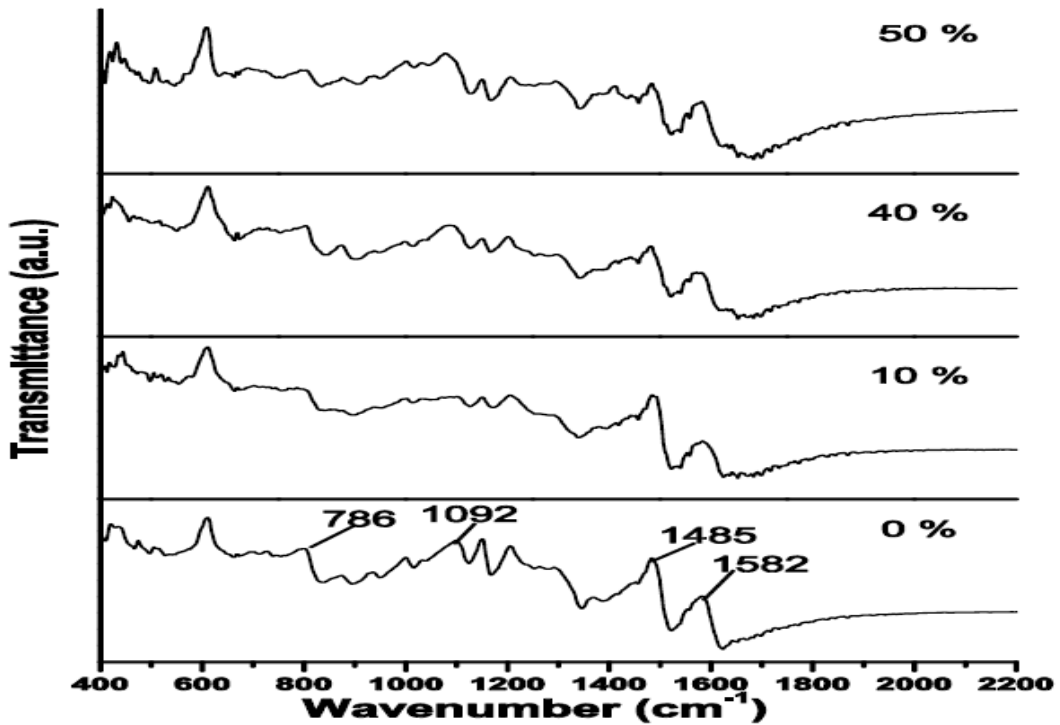


Figure 6: FTIR Pattern of POT at different Doping Concentrations of V<sub>2</sub>O<sub>5</sub>

Figure shows all the characteristic bands of POT. Bands observed in the range of 1574–1591  $\text{cm}^{-1}$  are the characteristic peaks of nitrogen quinoid ring, [32] whose broadening reduces with dopant concentration. According to the vibrational analysis of PANI and its derivatives, the position of this band can be taken as an indication of the degree of oxidation of the polymer. The origin of this band is due to the superposition of C–C stretching vibrations of the benzene ring. The characteristic peaks at around 1582  $\text{cm}^{-1}$  and 1485  $\text{cm}^{-1}$  are attributed to the stretching vibrations of N–Q and N–B–N rings respectively (where Q refers to Quinoid and B refers to Benzenoid ring). The band at 1485  $\text{cm}^{-1}$  is assigned to the C–H stretching of secondary aromatic

amine. The band at 1092  $\text{cm}^{-1}$  is attributed to the characteristic peak of B–NH–Q or B–NH–B bonds which are in plane bending modes. The out of plane bending deformations of C–H in the 1, 2, 4 substituted benzene ring are attributed to the band at 786  $\text{cm}^{-1}$ . The peaks obtained are in good agreement with the literature of POT [33, 34]. As the dopant concentration is increasing we can see the formation of alkynes corresponding to the wave number 1679–1687  $\text{cm}^{-1}$  which are weak, showing the C=C stretch. The alkyne group creation requires a huge reorganization of molecular bonds. The simultaneous C–C and C–H bond breaking is necessary to trigger the alkyne's formation. In the present case the electronic excitation energy values are above the threshold, which is necessary to trigger the alkyne formation. The delocalization of  $\pi$  electrons is also evident from the formation of triple bonds. Comparison of POT/ V<sub>2</sub>O<sub>5</sub> spectra with POT spectrum shows shift of peaks of Quinoid units from 1485  $\text{cm}^{-1}$  to 1476  $\text{cm}^{-1}$  and from 1092  $\text{cm}^{-1}$  to 1075  $\text{cm}^{-1}$ . The shift in the peak of FTIR spectra of V<sub>2</sub>O<sub>5</sub> doped POT is due to more ion formation after doping. After a doping of 10 % the alkyne formation takes place [35]. This indicates that the formation of triple bonds is affecting the semi conducting property of the doped polymer. So, although there is alkyne formation the semiconducting nature of the doped polymers is more.

### 3.4. XRD Studies

Figure 7 shows X-ray diffraction pattern of undoped and V<sub>2</sub>O<sub>5</sub> doped POT which confirms semi-crystalline nature of doped samples. XRD pattern of undoped sample of POT shows its amorphous nature. The DC conductivity increases due to the increase in crystallinity of the doped sample.

In undoped sample the amorphous hump at  $27.3^\circ$  is in accordance with the values found in the literature [10]. As the concentration of dopant increases, the crystallinity of polymer increases thus reducing the hump at  $27.3^\circ$  in the XRD pattern.

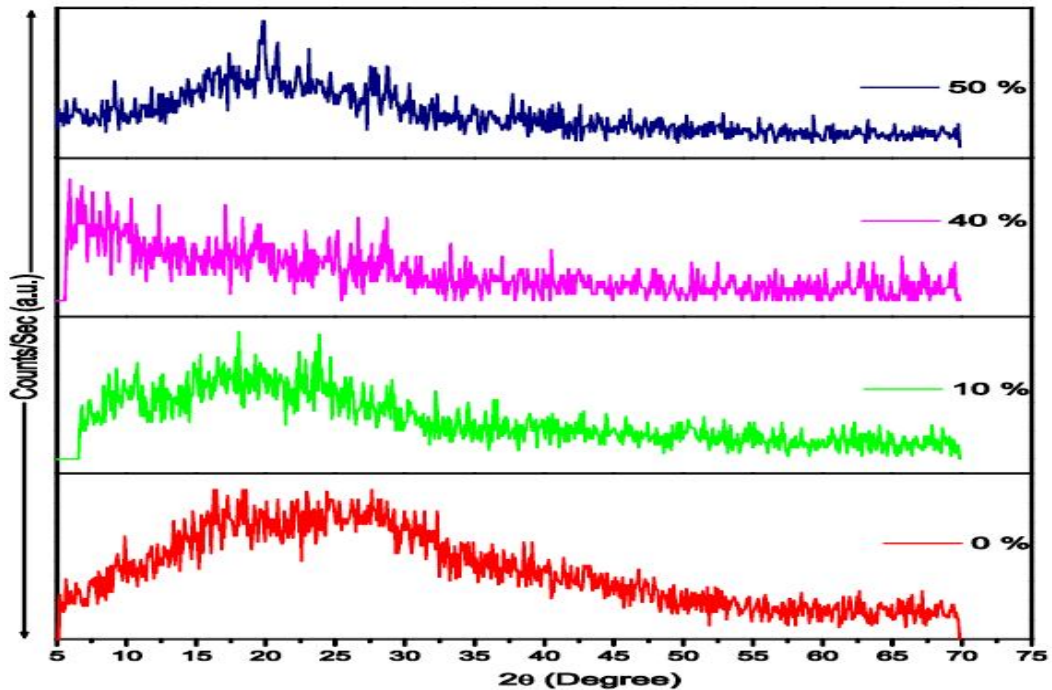


**Figure 7: The XRD Pattern of POT at different Doping Concentrations of  $V_2O_5$**

The increase in crystallinity of the composites after doping may be due to the systematic alignment of polymer chain folding or by the formation of single or multiple helices, for part of their length [25].

### 3.5. Photoluminescence Studies

The ability of a polymer to exhibit photoluminescence is associated with presence of dopant which may change with the concentration of the dopant [26]. The photoluminescence spectroscopy (PL) of POT and  $V_2O_5$  doped POT has been performed and is shown in Figure 8. The spectra of undoped POT shows only one peak at 549 nm confirming the oxidized phase of POT. There is a shift in this peak position in doped samples towards higher wavelength with change in concentration of the dopant.

It is also observed that PL peaks are broadened with increase in doping concentration. The relative intensity of emission peaks is also found to alter with different weight percentage of dopant (due to polarity).

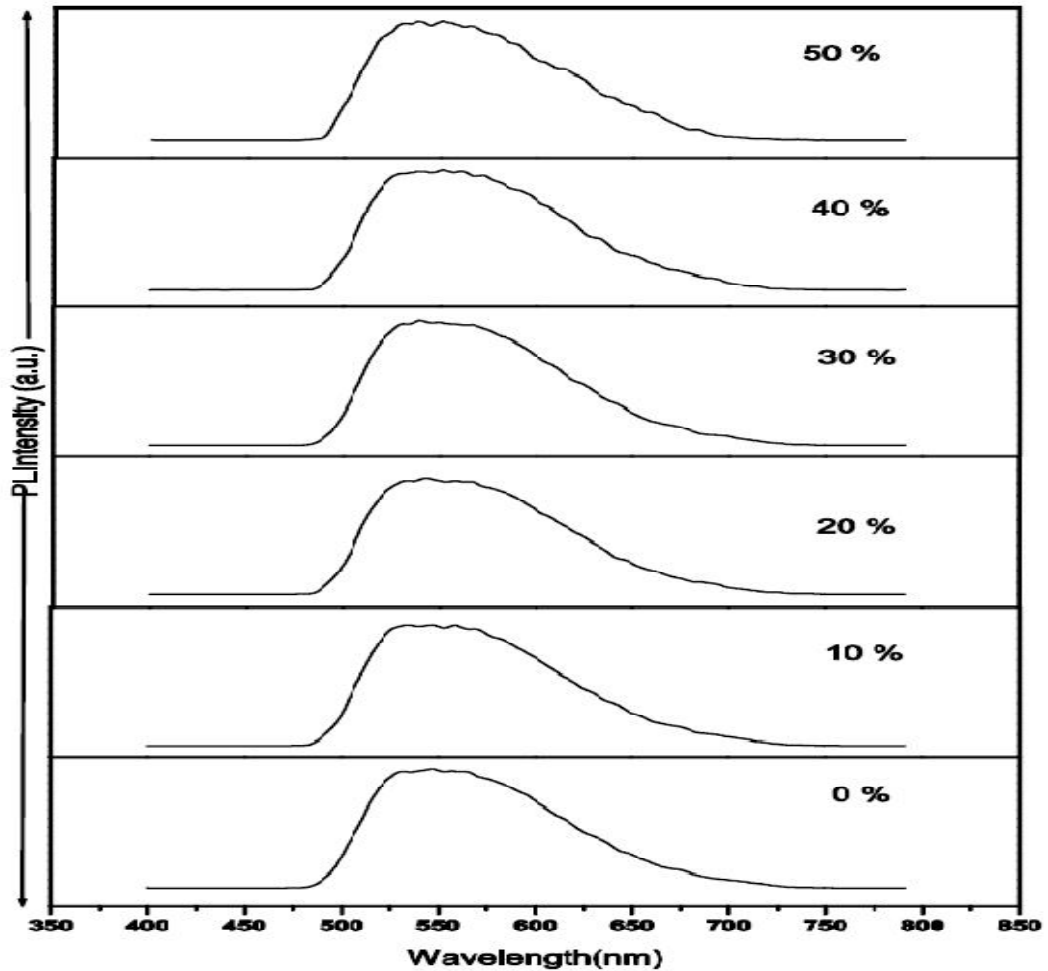


**Figure 8: Photoluminescence Spectra of POT at different Doping Concentrations of V<sub>2</sub>O<sub>5</sub>**

This may be due to interchain species, which plays an important role in the emission process of conjugated polymers. The intensity of peaks depends on factors such as polymer coil size, the nature of polymer-solvent, polymer-dopant interactions, and the degree of chain overlapping [36].

The PL spectra of samples have the same shape, which indicates that it is an efficient way to tune the intensities of the peak by employing specific dopant with different compositions (w/w).

#### 4. Conclusion

In the present communication, POT is successfully synthesized and doped with different weight percentage of  $V_2O_5$ . It has been observed that doping causes noticeable changes in the electrical and spectroscopic properties of POT. DC conductivity measurements show that the polymer composites are semi conducting in nature and there is an increase in conductivity after doping by three orders of magnitude. It is suggested that conduction is taking place due to a wide range of localized states present in the polymer composites. XRD studies of these polymer composites indicate increase in crystallinity after doping which may be correlated with a decrease in the band gap. FTIR spectra corroborate the structural changes of POT after doping of  $V_2O_5$  and also confirm the incorporation of  $V_2O_5$  in polymer chain. UV-Visible studies reveal the existence of indirect bandgap within the polymer which decreases after doping. Also the incorporation of the dopant causes systematic alignment of polymeric chains and increases delocalisation in the polymer matrix which lowers the band gap. These composites have been found to show high values of both real and imaginary parts of dielectric constant and loss. The doped polymers exhibit PL emission intensity which makes them suitable for use in various optoelectronic applications, such as polymer LEDs.

#### Acknowledgements

We also acknowledge Dr. Sukhveer Singh and his group (NPL) for FTIR Spectrophotometer. One of the authors (Shama Islam) acknowledges the financial support by the UGC.

#### References

- MacDiarmid, A.G., & Epstein A. J. (1994). *Frontiers of polymers and advanced materials.* (New York: Plenum Press) 251.
- MacDiarmid, A. G., & Epstein A. J. (1995). secondary doping in polyaniline. *Synth. Met.*, 69, 85.
- Kaiser, A. B., Subramaniam, C. K., Gilberd, P. W., & Wessling B. (1995). Systematic Conductivity Behavior in Conducting Polymers: Effects of Heterogeneous Disorder. *Synth. Met.*, 69, 197.

- Kaiser, A. B., Liu, C. J., Gilberd, P. W., Kemp, N. T., Wessling, B., Blaszkiewicz, M., McLachlan, D. S., & Newnham R. (1992). The volume fraction and temperature dependence of the resistivity in carbon black and graphite polymer composites: An effective media—percolation approach. *J. Polym. Eng. Sci.*, 32, 421.
- Angelopoulos, M., Ray, A., MacDiarmid, A. G., Epstein A. J. (1987). Polyaniline: Processability from aqueous solutions and effect of water vapor on conductivity. *Synth Met.*, 21, 12.
- Andreatta, A., Cao, Y., Chiang, J. C., Heeger, A. J., & Smith P. (1988). Electrically-conductive fibers of polyaniline spun from solutions in concentrated sulfuric acid. *Synth Met.*, 26, 383.
- Kumar, N., Vadera, S. R., Singh, J., Das, G., Negi, S. C., Aparna, P., & Tuli A. (1996). Conducting Polymers: Emerging Commercial Materials. *Def. Sci. J.*, 56, 91.
- Dao, L. H., Leclerc, M., Guay, J., & Chevalier J. W. (1989). Synthesis and characterization of substituted poly(anilines). *Synth Met. E*, 29, 377.
- D'Aparno, G., Leclerc, M., & Zotti G. (1993). *J. Electroanal Chem.*, 35, 145.
- Mortimer R. J. (1995). Electrochromic materials. *Mater Chem.*, 5 969.
- Datta, M., & Singhal, R. J., (2006). *Appl. Polym. Sci.*, 103, 3299.
- Chen, L. F., Ong, C. K., Neo, C. P., Varadan, V.V., & Varadan V. K. (2004). *Microwave electronics: Measurement and material characterization*. (England: John Wiley & Sons), 177.
- Dutta, P., Biswas, S., Ghosh, S., De, S. K., & Chatterjee S. (2001). The dc and ac conductivity of polyaniline–polyvinyl alcohol. blends *Synth. Met.*, 122, 455.
- Gangopadhyay, R., De, A., & Ghosh G. (2001). Polyaniline–poly(vinyl alcohol) conducting composite: material with easy processability and novel application potential. *Synth. Met.*, 123, 529.
- Saad, A. A., Khan, W., Dhiman, P. & Naqvi A. H. (2013). Structural, Optical and Magnetic Properties of Perovskite (La<sub>1-x</sub>Sr<sub>x</sub>)(Fe<sub>1-x</sub>Ni<sub>x</sub>)O<sub>3</sub>, (x = 0.0, 0.1 & 0. 2) Nanoparticles. *Electronic Materials Letters.*, 9, 77.
- Murugesan, R., & Subramanian E. (2003). Charge dynamics in conducting polyaniline–metal oxalate composites. *Bull. Mater., Sci.* 26, 529.
- Troung, V. T., Codd, A. R., & Forsyth M. (1994). Dielectric-properties of conducting polymer composites at microwave-frequencies. *J. Mater. Sci.*, 29, 4331.
- Brosseau, C., Queffelec, P., & Talbot P. (2001). Microwave characterization of filled polymers. *J. Appl. Phys.*, 89, 4532.
- Rana, O., Srivastava, R., Chauhan, G., Zulfequar, M., Husain, M., Srivastava, P. C., & Kamalasanan M. N. (2012). Modification of metal–organic interface using F4-TCNQ for enhanced hole injection properties in optoelectronic devices. *Phys. Status Solidi A*, 209, 2539
- Majeed Khan, M. A., Zulfequar, M., Kumar, A. & Husain M. (2004). Conduction mechanism in amorphous Se<sub>75</sub>In<sub>25</sub>-xPbx films. *Mater. Chem. Phys.*, 87, 179.
- Kido, J., Endo, J., Nakada, T., Mori, T., Yokoi, A., & Matsumoto T. Extended Abstract (49th Spring Meeting, 2002), *Jpn. Soc. Appl. Phys.*, p. 1308 [in Japanese].
- Kido, J., Matsumoto, T., Nakada, T., Endo, J., Mori K., Kawamura N. & Yokoi A. (2003). High Efficiency Organic EL Devices having Charge Generation Layers. *SID Int. Symp. Dig. Tech.*, 34, 964.

- Lakshmi, G. B. V. S., Avasthi, D. K., Jai Prakash, Siddiqui, A. M., Ali, V., Khan, S. A., & Zulfequar M. (2011). Structural, optical and gas evolution studies of 60 MeV Si<sup>5+</sup> ion irradiated PoT-PVC blends. *Adv. Mat. Lett.*, 2(2), 125-130.
- Heeger, A. J., Kivelson, S., Schrieffer, J. R., & Su W. P. (1988). *Rev. Mod. Phys.*, 60, 781.
- Zishan, H. Khan, Malik, M. M., Zulfequar, M., & Husain M. (1995). Electrical conduction mechanism in a-Se<sub>80-x</sub>Te<sub>20</sub> films (0<or=x<or=20). *J. phy. Cond. Matter.*, 7, 8979–8991.
- Mott, N. F., & Davis E. A. (1979). *Electronics Processes in Non-Crystalline Materials*. Clarendon, Oxford, 428.
- Ghiordanescu, V., Sina, M., Neldelcu, M. & Giubelan M. J. (2001). *Optoelectron. Adv. M.*, 3, 89.
- Mott, N. F., & Davis E. A. (1970). Conduction in non-Crystalline systems. *Philos. Mag.*, 22, 7.
- Lakshmi, G. B. V. S., Ali, V., Siddiqui, A. M., Kulriya, P. K., & Zulfequar M. (2008). RF-plasma polymerization and characterization of polyaniline. *European Physical Journal, Applied Physics*, 39(3), 251.
- Tauc, J., Grigirovici, R., & Vancu A. (1996). *Phys. Status Solidi*, 15, 627.
- Shamshad, A. Khan, Zulfequar, M., & Hussain M. (2005). Optical band gap and optical constants in a-Se<sub>80</sub>Te<sub>20-x</sub>Pb<sub>x</sub> thin films. *Current Applied Physics*, 5, 583.
- Mallick, K., Witcomb, M. J., & Scurrill M. S. (2006). In situ synthesis of copper nanoparticles and poly(o-toluidine): a metal-polymer composite material. *Eur. Polym. J.*, 42, 670.
- Saravanan, S., Joseph Mathai, C., Venkatachalam, S., & Anatharaman M. R. (2004). *New J Phys*, 664.
- Fink, J., & Leising G. (1991). *Physical Review B*, 15, 2022-2025.
- Ameen, S., Ali, V., Zulfequar, M., Haq, M. M., & Husain M. (2009). Preparation and measurements of electrical and spectroscopic properties of sodium thiosulphate doped polyaniline. *Current Applied Physics*, 9, 2.
- Antonel, P. S., Molina, F. V., & Andrade E. M. (2007). Fluorescence of polyaniline films on platinum surfaces. Influence of redox state and conductive domains. *J. Electroanal. Chem.*, 599, 52.